Multiple roles of PPARα in brown adipose tissue under constitutive and cold conditions

Makiko Komatsu[1,2], Yuhong Tong[1], Yufeng Li[1], Takero Nakajima[1], Gang Li[1,3], Rui Hu[1,4], Eiko Sugiyama[1,5], Yuji Kamijo[1,6], Naoki Tanaka[1], Atsushi Hara[1]*, and Toshifumi Aoyama[1]

[1]Department of Metabolic Regulation, Institute on Aging and Adaptation, Shinshu University Graduate School of Medicine, 3-1-1 Asahi, Matsumoto, Nagano 390-8621, Japan

[2]School of Nursing & Health, Aichi prefectural University, kamishidami, Moriyama-ku, Nagoya, Aichi 463-8502, Japan

[3]Cardiac Center of Hebei Provincial People's Hospital, 348 Hepingxi Road, Shijiazhuang, Hebei, 050051, People's Republic of China

[4]The Second Hospital of Hebei Medical University, 205 Heping Road, Shijiazhuang, Hebei, 050011, People's Republic of China

[5]Department of Nutritional Science, Nagano Prefectural College, Nagano 380-8525, Japan

[6]Department of Internal Medicine, Shinshu University School of Medicine, 3-1-1 Asahi, Matsumoto, Nagano 390-8621, Japan

* To whom correspondence should be addressed:

E-mail:kareisei@shinshu-u.ac.jp

Fax: 81-263-37-3094; Tel.: 81-263-37-2850

Running title: Regulation of energy production by PPARα

Total character count: 35,834 including spaces

Abstract

Peroxisome proliferator-activated receptor α (PPARα) is a member of the nuclear receptor family, regulating fatty acid degradation in many organs. Two-dimensional SDS-PAGE of brown adipose tissue (BAT) from PPARα-null mice produced a higher-density spot. Proteomic analysis indicated that the protein was pyruvate dehydrogenase β (PDHβ). To observe PDHβ regulation in BAT, the organ was stimulated by long-term cold exposure, and the activities of associated enzymes were investigated. Histological and biochemical analyses of BAT showed a significant decrease in the triglyceride content in wild-type mice and some degree of decrease in PPARα-null mice on cold exposure. Analyses of molecules related to glucose metabolism revealed that the expression of PDHβ is under PPARα-specific regulation, and that glucose degradation ability may decrease on cold exposure. On the other hand, analyses of molecules related to fatty acid metabolism showed that numerous PPARα/γ target molecules are induced on cold exposure, and that fatty acid degradation ability in wild-type mice is markedly enhanced and also increases to same degree in PPARα-null mice on cold exposure. Thus, this study proposes novel and multiple roles of PPARα in BAT.

Introduction

BAT consumes energy for thermogenesis in response to cold or overfeeding (Guardiola-Diaz *et al*., 1999; Cannon & Nedergaard, 2004). BAT contains abundant mitochondria for this function, and mitochondrial fatty acid β-oxidation enzymes are expressed at a high level (Guardiola-Diaz *et al*., 1999). It has been reported that the BAT weight and peroxisome proliferator-activated receptor γ coactivator-1α (PGC-1α) mRNA in BAT increase upon cold exposure (Guardiola-Diaz *et al*., 1999; Puigserver *et al*., 1998). PGC-1α activates the expression of uncoupling protein 1 (UCP 1) present in the inner mitochondrial membrane and mitochondrial enzymes of the respiratory chain, leading to non-shivering thermogenesis (Daikoku *et al*., 2000; Guardiola-Diaz *et al*., 1999; Puigserver *et al*., 1998; Vega & Kelly, 1997). It is well-known that ATP production or thermogenesis in BAT mostly occurs in mitochondria, and the energy source is supplied mainly via 2 pathways: one pathway takes up and breaks down glucose, and the other breaks down fatty acids/triglycerides from the blood stream or triglycerides stored in BAT cells. Pyruvate dehydrogenases (PDH) α and β and pyruvate dehydrogenase kinases (PDK) 2 and 4 play a central role in the former pathway that supplies energy from glucose (An & Rodrigues, 2006; Huang *et al*., 2002). In the latter pathway that supplies energy from lipids, many proteins are involved. For example, fatty acid translocase (FAT), fatty acid transport protein (FATP), and lipoprotein lipase (LPL) incorporate fatty acids from blood, and these incorporated fatty acids are degraded by long-chain acyl-CoA synthetase (LACS), carnitine palmitoyltransferase 1 (CPT1b), and various β-oxidation enzymes (An & Rodrigues, 2006). PPARα belongs to the steroid/nuclear receptor superfamily, and has various functions that are associated with the regulation of lipid transport, storage, and metabolism, influencing a variety of events in cells (Desvergne & Wahli, 1999; Mandard *et al*., 2004; Vega *et al*., 2000). PPARα is also known to be involved in glucose degradation by enhancing the mRNA expression of PDK4 in the former pathway in the liver and muscle (Huang *et al*., 2002; Motojima & Seto, 2003; Muoio *et al*., 2002). We have also reported that PPARα is closely associated with the transcriptional regulation of many proteins in the latter pathway involved in fatty acid/triglyceride degradation in the liver,

muscle, and kidney (Aoyama *et al*., 1998; Aoyama *et al*., 1995; Aoyama *et al*., 1993; Aoyama *et al*., 1989; Kamijo *et al*., 2007; Nakajima *et al*., 2004; Tanaka *et al*., 2008). However, there have been fewer reports on the specific physiological roles of PPARα in BAT (Barbera *et al*., 2001; Tong *et al*., 2005; Goetzman *et al*., 2005; Guardiola-Diaz *et al*., 1999). Moreover, on cold exposure, many other factors participate in the transcription of proteins in the latter pathway involved in fatty acid/triglyceride degradation (Vega & Kelly, 1997; Puigserver *et al*., 1998; Guardiola-Diaz *et al*., 1999; Daikoku *et al*., 2000; Lehman *et al*., 2000), and the role of PPARα has not been fully elucidated in BAT. We partially clarified the physiological function of PPARα in BAT using PPARα-null mice in a previous study (Tong *et al*., 2005), in which a heavy spot not synchronously altered was detected on SDS-PAGE analysis. In this paper, the protein was extracted from the spot and identified as PDHβ, involved in glucose degradation in the former pathway, on analysis by MALDI-TOF-MS. To understand the significance of the changes in BAT in detail, we analyzed the regulation of representative proteins in both the glucose- and lipid-derived energy production systems in the mice under long-term cold exposure, and discovered an unexpected and interesting phenomenon. Thus, we partially clarified the specific role of PPARα in BAT based on these findings.

Results

Protein identification by MALDI-TOF-MS

The results of two-dimensional (2D) SDS-PAGE analysis of interscapular BAT proteins (23ºC) are shown in Fig. 1A. An intense spot, showing behavior different from the five synchronous spots reported in our previous study (Tong *et al*., 2005), was detected in PPARα-null mice. The spot was analyzed by MALDI-TOF-MS after digestion with trypsin, as previously reported (Tong *et al*., 2005). The mass spectrum of peptides obtained from the spot is shown in Fig. 1B. The peptide pattern from this analysis was subjected to database analysis using MS-Fit, and the protein was identified as a PDHβ subunit (Swiss-Prot, Q9D051), with a concordance rate of 80.5% (Fig. 1A, B).

Histological analysis and fatty acid degradation ability

PDH is an enzyme of the mitochondrial energy production system that uses glucose as a substrate. We attempted to clarify the function of PDH in BAT via BAT activation. BAT is usually activated by cold exposure in mature mice, and actively produces heat to maintain the body temperature. Wild-type and PPARα-null mice were maintained under long-term cold exposure. In most studies reported thus far on cold exposure, the exposure period was relatively short: several hours to about 2 days, and responses in the early phase of cold acclimatization were investigated (Puigserver *et al*., 1998; Guardiola-Diaz *et al*., 1999; Daikoku *et al*., 2000; Yu *et al*., 2002; Goetzman *et al*., 2005). However, we set a 12-week, long-term cold exposure period to observe BAT function in a steady state in which the animals had fully adapted to the cold condition. The results are shown in Fig. 2A. The BAT weight increased with time in both PPARα-null and wild-type mice, and stabilized after 4 weeks. BAT was histologically analyzed at each time point. At 4, 8, and 12 weeks, lipid droplets were markedly reduced in wild-type compared to PPARα-null mice. Typical BAT in a stable state at 8 weeks is shown in Fig. 2B. In BAT in PPARα-null and wild-type mice maintained at 23ºC, lipid droplets were similarly abundant, and it was difficult to histologically distinguish the two groups. In contrast, the size of

lipid droplets in BAT markedly shrank in wild-type mice maintained at 4ºC, compared to that at 23ºC. This shrinkage is probably ascribed to the consumption of triglycerides in the lipid droplets. However, in PPARα-null mice maintained at 4ºC, this shrinkage was not noted. To biochemically investigate these histological findings, the triglyceride content of BAT was measured (Fig. 2C). At 8 weeks of cold exposure, the triglyceride content of BAT was markedly decreased in wild-type mice maintained at 4ºC, compared to that at 23ºC. In PPARα-null mice maintained at 4ºC, the content was decreased slightly. The alterations in the triglyceride content were consistent with the histological changes shown in Fig. 2B, indicating that PPARα is closely involved in the control of triglyceride/fatty acid metabolism. The findings of 2D SDS-PAGE analysis suggested that PPARα suppresses PDHβ expression in BAT in wild-type mice. Based on these findings, PPARα may be involved in the regulation of two metabolic systems, fatty acid and glucose degradation. Thus, we investigated the expression of typical proteins involved in these metabolic systems.

mRNA analyses

The mRNA expressions of important enzymes in the glucose degradation system are shown in Figs. 3A and 3B. The PDHα expression level was not significantly different between PPARα-null and wild-type mice. Cold exposure only slightly increased the mRNA content in both groups, showing no marked effect. PDHβ expression reflected the findings of 2D SDS-PAGE analysis, revealing a markedly higher mRNA content in PPARα-null than in wild-type mice under both constitutive and cold conditions. In contrast, the expressions of PDH enzyme complex-inactivating enzymes, PDK2 and PDK4, were not significantly different between PPARα-null and wild-type mice under either the constitutive or cold condition, but the mRNA contents of both enzymes markedly increased on cold exposure (Fig. 3A). The mRNA expressions of pyruvate carboxylase (PC), muscle type pyruvate kinase (M-PK), and hexokinase II (HK-II) were respectively unchanged under all conditions examined (Fig. 3B). Next, PDH activity was measured to confirm whether the changes at the mRNA level were reflected in PDH

function. PDH activity was reduced on cold exposure, as shown in Fig. 3C, which may be partially due to the increases in the mRNA contents of PDK2 and PDK4. PDH activity was higher in PPARα-null than in wild-type mice under both constitutive and cold conditions, which may depend on the PPARα-dependent suppression of PDHβ expression.

The expression of important proteins in the fatty acid-metabolizing system was then analyzed. The mRNA contents of several fatty acid β-oxidation proteins, LACS, CPT1b, and medium-chain acyl-CoA dehydrogenase (MCAD), were higher in wild-type than in PPARα-null mice under the constitutive condition. These contents significantly increased on cold exposure both in wild-type and PPARα-null mice (Fig. 4A). The changes in palmitic acid β-oxidation activity (Fig. 4B) were well consistent with those in the mRNA level (Fig. 4A). The mRNA contents of the key proteins, FAT, FATP, and LPL, in the fatty acid uptake system were not significantly different between wild-type and PPARα-null mice under the constitutive condition. The contents of the three key proteins in wild-type mice and those of FATP and LPL in PPARα-null mice markedly increased on cold exposure (Fig. 4C). However, the mRNA contents of fatty acid-synthesizing enzymes, acetyl-CoA carboxylase (ACC-1) and fatty acid synthase (FAS), were not different between wild-type and PPARα-null mice under either the constitutive or cold condition (Fig. 4D). These changes in fatty acid β-oxidation and fatty acid uptake systems suggest the intensive enhancement of fatty acid degradation ability in wild-type mice and enhancement to some degree in PPARα-null mice on cold exposure. Since LACS, CPT1b, MCAD, FAT, FATP, and LPL are known to be target gene products of PPARα and/or PPARγ (Aoyama *et al*., 1998; Mandard *et al*., 2004), and PGC-1α is involved in thermogenesis through the function of PPARα in BAT (Lehman *et al*., 2000), the PPARα, PPARγ, and PGC-1α mRNA levels were examined (Fig. 4E). The mRNA content of PPARα in wild-type mice was unchanged on cold exposure. The level of PPARγ mRNA was not different between wild-type and PPARα-null mice, and was not altered on cold exposure. However, the level of PGC-1α mRNA was markedly increased under the cold condition in both wild-type and PPARα-null mice, suggesting that the transcriptional induction of the six PPARα/γ target gene products on cold

exposure occurred through the increase of PGC-1α, at least in part. In addition, the content of hepatocyte nuclear factor 4α (HNF4α) mRNA was investigated (Fig. 4E), since the PPARα complex can compete with the HNF4α complex at the binding site of the HNF4α target gene such as apolipoprotein CIII (Hertz *et al*., 1995). The level of HNF4α mRNA was not different between wild-type and PPARα-null mice, and was not changed on cold exposure.

Discussion

In most previous reports concerning cold exposure, the period of exposure was short, being several hours to weeks (Daikoku *et al*., 2000; Goetzman *et al*., 2005; Guardiola-Diaz *et al*., 1999; Puigserver *et al*., 1998; Yu *et al*., 2002). The expression levels of many proteins including PPARα/γ dizzily changed during several weeks of cold exposure (Guardiola-Diaz *et al*., 1999). We exposed mice to cold conditions for more than 6 weeks, with the levels of most factors becoming constant before 12 weeks. When analyzing BAT samples from mice exposed to cold conditions for 0 and 12 weeks, respectively, we obtained novel results: a marked reduction of the triglyceride content in BAT from wild-type mice exposed 4ºC and some reduction of that in PPARα-null mice. After completing a series of analyses, the following mechanisms are proposed. In wild-type mice, the mRNA levels of three β-oxidation enzymes and three proteins in the fatty acid uptake system significantly increased on cold exposure, suggesting the intensive enhancement of fatty acid degradation ability. In PPARα-null mice, all proteins except FAT increased to some extent, also suggesting some level of enhancement. These results are well compatible with the changes in the triglyceride content described above. Since these six proteins are known to be PPARα target gene products (Aoyama *et al*., 1998; Mandard *et al*., 2004), their synchronous increases are probably due to the functional activation of PPARα. Since FATP and LPL are also known to be PPARγ target gene products (Martin G *et al*., 1997; Schoonjans K *et al*., 1996), their increases in PPARα-null mice are possibly dependent on that of PPARγ. The synchronous increases of the three β-oxidation enzymes in PPARα-null mice are believed to relate to that of PPARγ, although the detailed mechanisms are hitherto unknown. PPARα/γ activation under the cold condition seem to be caused by the increase of PGC-1α, which is consistent with previous observations (Lehman *et al*., 2000).

On the other hand, we obtained novel results concerning PDH activity. The changes in PDH activity were probably derived from the PPARα-specific suppression of PDHβ and cold exposure-dependent induction of PDK2/4. In the former, the participation of HNF4α was noted in numerous mechanisms with PPARα-related suppression (Hertz *et al*., 1995; Mandard *et al*.,

2004). The upstream region of the PDHβ gene was searched (Gupta *et al*., 2005; Podvinec *et al*., 2002), and the presence of a region showing a close homology to the HNF4α-binding site was confirmed (ggtccagagttca: -1,069～-1,057). At this site, the activated PPARα may compete for binding with HNF4α, a positive regulator, resulting in suppression. In the latter, the PPARα/γ activation under the cold condition mentioned above contributes to the induction of PDK2/4, target gene products of PPARα (Mandard *et al*., 2004), although the specific mechanisms are still unknown. The decrease in PDH activity under the cold condition may lower glucose degradation ability, which requires further study for confirmation. Taken together, this study proposes unexpected and multiple roles of PPARα in BAT under long-term cold exposure.

While exposing wild-type mice to 4ºC for 8 weeks: BAT weight increased 2.5 fold in a PPARα-independent manner; the palmitic acid β-oxidation activity increased 2.3 fold; and the ability in fatty acid uptake was significantly enhanced, however, these changes did not occur in the liver. In our calculation, the fatty acid β-oxidation ability in whole BAT reached about 65% of that of the whole liver. These results suggest that BAT under long-term cold exposure can markedly influence the metabolism of fatty acids/triglycerides throughout the entire body. Very recently, the presence of active BAT was confirmed in adults (Cypess *et al*., 2009), and the findings in this study may therefore contribute to human health, particularly in the fields of fatty liver, hypertriglyceridemia, and diabetes.

Experimental procedures

Materials and chemicals

Immobiline DryStrips (pH 3-10, 18 cm) were purchased from GE Healthcare Bioscience Co., USA. Montage In-Gel Digest$_{96}$ Kit and ZipTip$_{C18}$ were from Millipore (Bedford, MA, USA). Adrenocorticotropic hormone (ACTH) fragment 7-38, α-cyano-4-hydroxy cinnamic acid (α-CHCA), and angiotensin I (human) were from Sigma (St. Louis, MO, USA). Iodoacetamide and dithiothreitol (DTT) were from Nacalai Tesque (Kyoto, Japan). 1-Step NBT/BCIP (nitro blue tetrazolium/5-bromo-4-chloro-3-indolylphosphate) was from Pierce (Rockford, IL, USA). [1-^{14}C]Palmitic acid (54 mCi/mmol) was from American Radiolabeled Chemicals (St. Louis, MO, USA). All other reagents were of the highest grade available in Japan.

Animals and experimental treatments

PPARα-null mice with an Sv/129 genetic background were produced as described elsewhere (Lee *et al*., 1995). Wild-type Sv/129 mice were used as controls in all experiments. In some experiments, 16-week-old mice were kept in a cold room (4ºC) for 12 weeks.

2D SDS-PAGE

BAT was homogenized in a gel-swelling reagent containing urea, DTT, Pharmalyte 3-10, acetic acid, Orange G, and Triton X-100 (Toda, 2000). The supernatant was obtained by centrifugation (15,200×g, 30 min) at 4ºC and used for 2D SDS-PAGE. In brief, the protein samples obtained from 5 to 20 mg tissue were loaded on a re-swollen Immobiline DryStrip, respectively. Then, isoelectric focusing was carried out at 20ºC. After the gel strips were equilibrated with the SDS-treatment solution, the proteins were separated by SDS-PAGE using 200 mM Tris-HCl (pH 8.8) for the anodic electrode buffer and 100 mM Tris-Tricine for the cathodic electrode buffer at 30 mA for 4 h at 20ºC. The samples of PPARα-null mice and wild-type controls were simultaneously analyzed using the same apparatus (O'Farrell, 1975).

In-gel digestion

The protein spot separated by 2D SDS-PAGE was excised from the gel after staining with Coomassie brilliant blue R-250 and digested using a Montage In-Gel $Digest_{96}$ Kit based on the methods according to the manufacturer's protocol (http://www.millipore.com/userguides.nsf/docs/P36379). Briefly, the protein embedded in the gel was digested overnight at 30ºC using trypsin in ammonium bicarbonate buffer. Peptides were extracted from the gels with trifluoroacetic acid-containing acetonitrile and purified with $ZipTip_{C18}$. Finally, the purified peptides were analyzed with α-CHCA by MALDI-TOF-MS as follows.

MALDI-TOF-MS

A Voyager Elite XL Biospectrometry workstation (PerSeptive Biosystem, Framingham, MA, USA) equipped with a delayed extraction ion source was used for MALDI-TOF-MS analysis in the reflector mode with the following parameters: accelerating voltage, 22 kV; grid voltage, 80% of the accelerating voltage; guide wire voltage, 0.05% of the accelerating voltage; delay time, 200 ns. A nitrogen laser (337 nm) was used for ionization. The calibration was performed with the monoisotopic peaks of the dimer of α-CHCA (379.0930 m/z), angiotensin I (1,296.6853 m/z), and ACTH (7-38 clip) (3,657.9294 m/z).

Database searching

Peptide mass data from MALDI-TOF-MS were subjected to a database search using MS-Fit, a typical peptide mass fingerprinting program on the web site of the University of California, San Francisco (http://prospector.ucsf.edu/).

Morphological analysis

Small sections of BAT from each mouse were fixed in 10% buffered formalin, and the sections were stained with hematoxylin and eosin (H&E), as described previously (Watanabe *et al*., 2000).

Triglyceride determination

Triglyceride concentrations were measured using a kit purchased from Wako (Osaka, Japan) based on the methods according to the manufacturer's protocol.

Pyruvate dehydrogenase activity

PDH activity was measured using the method of Hinman and Blass (Hinman & Blass, 1981). The assay for the pyruvate dehydrogenase complex measures NADH production by coupling it to the reduction of a tetrazolium dye via an intermediate electron carrier. The reaction mixture contained tissue homogenate, 0.6 mM 2-(p-iodophenyl)-3-p-nitrophenyl-5-phenyl-tetrazolium chloride, 22.5 mM NAD, 0.2 mM thiamin pyrophosphate, 0.1 mM coenzyme A, 0.3 mM dithiothreitol, 5 mM pyruvate, 1 mM magnesium chloride, and 1 mg/ml of BSA in 0.05 M potassium phosphate buffer, pH 7.8.

Analysis of mRNA

Total RNA was isolated from BAT using the RNeasy Mini kit (Qiagen GmbH., Hilden, Germany). RNA was treated with RNase-free DNase (Qiagen), and reverse transcribed using oligo-dT primer (SuperScript First-Strand Synthesis System, Invitrogen Life Technologies, Carlsbad, CA, USA) to a final concentration of 20 ng/μl. We designed gene-specific primers using Primer Express Software (Applied Biosystems, USA). Each standard plasmid DNA for real-time quantitative PCR was constructed using pGEM-T Easy Vector System I and the Wizard Plus SV Minipreps DNA Purification System (Promega Co., Madison, WI, USA). Real-time PCR was performed using the SYBR Green Master Mix (Applied Biosystems, Foster City, CA, USA) with the ABI Prism 7700 Sequence Detection System. Each sample was analyzed in triplicate with 25-ng templates and a final 0.4 μM of each primer set. Cycling conditions were set at 50ºC for 2 min, 95ºC for 10 min, followed by 40 cycles at 95ºC for 15 s and 60ºC for 1 min. All real-time PCR data were standardized with the value of a housekeeping gene, glyceraldehyde-3-phosphate dehydrogenase (GAPDH). The primer sets used were as follows: 5'-aatcccacggatcacgtcat-3' and 5'-tcctttgcgtccagtcagct-3' for PDHα (GenBank Accession number NM_008811);

5’-aaggaggctggccacaattt-3’ and 5’-gggcatcaaggaagttgaatg-3’ for PDHβ (NM_024221);

5’-ccgttgtccatgaagcagttt-3’ and 5’-cctgccggaggaaagtgaa-3’ for PDK2 (NM_133667);

5’-agaagaccagaaagccctgtca-3’ and 5’-gccattgtagggaccacattatg-3’ for PDK4 (NM_013743);

5’-tcctacggcagtgatctggtg-3’ and 5’-ggttgcctgtagttccacttgtg-3’ for LACS (NM_007981);

5’-ccaaacgtcactgcctaagct-3’ and 5’-ctccatgcggtaatatgcttca-3’ for CPT1b (NM_009948);

5’-tgcttttgatagaaccagacctacagt-3’ and 5’-cttggtgctccactagcagctt-3’ for MCAD (NM_007382);

5’-ccaaatgaagatgagcataggacat-3’ and 5’-gttgacctgcagtcgttttgc-3’ for FAT (NM_007643);

5’-accaccgggcttcctaagg-3’ and 5’- ctgtaggaatggtggccaaag-3’ for FATP (NM_011977);

5’-cgctccattcatctcttcatt-3’ and 5’-ggcagagccctttctcaaagg-3’ for LPL (NM_63335);

5’-cctcagggtaccactacggagt-3’ and 5’-gccgaatagttcgccgaa-3’ for PPARα (NM_011144);

5’-ttccactatggagttcatgcttgt-3’ and 5’-tccggcagttaagatcacaccta-3’ for PPARγ (NM_011146);

5’-attttgatagtttactgaag-3’ and 5’-ctcacatgtgtacatatgta-3’ for PGC-1α (NM_008904);

5’-gggcacagaccgtggtagtt-3’ and 5’-caggatcagctgggatactgagt-3’ for ACC-1 (NM_193604);

5’-atcctggaacgagaacacgatct-3’ and 5’-agagacgtgtcactcctggactt-3’ for FAS (NM_007988);

5’-caagaggtccatggtgtttaagg-3’ and 5’-ggatggacacacggctcatg-3’ for HNF4α (NM_008261);

5’-acgtctcaccagtgactctgtca-3’ and 5’-agtagtgcttgccgtgcttgt-3’ for PC (NM_008797);

5’-atgtggctcggctgaatttc-3’ and 5’-ggtagagaatgggatcagatgca-3’ for M-PK (NM_011099);

5’-caaccaaaaccaagtgcagaag-3’ and 5’-tgctgtagggtgtgtgggagct-3’ for HK-II (NM_013820). The GAPDH primer set was purchased from Applied Biosystems.

Palmitic acid β-oxidation activity

Palmitic acid β-oxidation activity was measured as follows (Shindo *et al*., 1978). Briefly, the unfrozen BAT was homogenized in four volumes of 0.25 M sucrose containing 1 mM EDTA. The homogenate was incubated with the assay medium containing 50 μM [1-^{14}C]palmitic acid. The reaction was run for 30 min at 25ºC and stopped by the addition of perchloric acid. The mixture was centrifuged at 2,000 ×*g* for 10 min, and the unreacted palmitic acid in the supernatant was removed with three extraction of n-hexane. Radioactive degradation products

(acetic acid, acetyl-CoA, acetyl-carnitine, and intermediates in Krebs cycle etc.) were counted.

Statistical analysis

Analysis of significant differences with respect to the interactive effects of two factors (PPARα gene status and cold acclimatization treatment) was performed using a two-way ANOVA. Probability (*P*) values less than 0.05 were regarded as significant.

References

An, D. & Rodrigues, B. (2006) Role of changes in cardiac metabolism in development of diabetic cardiomyopathy. *Am. J. Heart Circ. Physiol.* **291**, 1489-1506.

Aoyama, T., Peters, J.M., Iritani, N., Nakajima, T., Furihata, K., Hashimoto, T. & Gonzalez, F.J. (1998) Altered constitutive expression of fatty acid-metabolizing enzymes in mice lacking the peroxisome proliferator-activated receptor alpha (PPARalpha). *J. Biol. Chem.* **273**, 5678-5684.

Aoyama, T., Souri, M., Ushikubo, S., Kamijo, T., Yamaguchi, S., Kelley, R.I., Rhead, W.J., Uetake, K., Tanaka, K. & Hashimoto, T. (1995) Purification of human very-long-chain acyl-coenzyme A dehydrogenase and characterization of its deficiency in seven patients. *J. Clin. Invest.* **95**, 2465-73.

Aoyama, T., Uchida, Y., Kelley, R.I., Marble, M., Hofman, K., Tonsgard, J.H., Rhead, W.J. & Hashimoto, T. (1993) A novel disease with deficiency of mitochondrial very-long-chain acyl-CoA dehydrogenase. *Biochem. Biophys. Res. Commun.* **191**, 1369-1372.

Aoyama, T., Yamano, S., Waxman, D.J., Lapenson, D.P., Meyer, U.A., Fischer, V., Tyndale, R., Inaba, T., Kalow, W., Gelboin, H.V., & Gonzalez, F.J. (1989) Cytochrome P-450 hPCN3, a novel cytochrome P-450 IIIA gene product that is differentially expressed in adult human liver. cDNA and deduced amino acid sequence and distinct specificities of cDNA-expressed hPCN1 and hPCN3 for the metabolism of steroid hormones and cyclosporine. *J. Biol. Chem.* **264**, 10388-95.

Barbera, M.J., Schluter, A., Pedraza, N., Iglesias, R., Villarroya, F. & Giralt, M. (2001) Peroxisome proliferator-activated receptor alpha activates transcription of the brown fat uncoupling protein-1 gene. A link between regulation of the thermogenic and lipid oxidation pathways in the brown fat cell. *J. Biol. Chem.* **276**, 1486-1493.

Cannon, B. & Nedergaard, J. (2004) Brown adipose tissue: function and physiological significance. *Physiol. Rev.* **84**, 277-359.

Cypess, A.M., Lehman, S., Williams, G., Tal, I., Rodman, D., Goldfine, A.B., Kuo, F.C., Palmer, E.L., Tseng, Y.H., Doria, A., Kolodny, G.M. & Kahn, C.R. (2009) Identification and importance

of brown adipose tissue in adult humans. *N. Engl. J. Med.* **360**, 1509-1517.

Daikoku, T., Shinohara, Y., Shima, A., Yamazaki, N. & Terada, H. (2000) Specific elevation of transcript levels of particular protein subtypes induced in brown adipose tissue by cold exposure. *Biochim. Biophys. Acta.* **1457**, 263-272.

Desvergne, B. & Wahli, W. (1999) Peroxisome proliferator-activated receptors: nuclear control of metabolism. *Endocr. Rev.* **20**, 649-688.

Goetzman, E.S., Tian, L. & Wood, P.A. (2005) Differential induction of genes in liver and brown adipose tissue regulated by peroxisome proliferator-activated receptor-alpha during fasting and cold exposure in acyl-CoA dehydrogenase-deficient mice. *Mol. Genet. Metab.* **84**, 39-47.

Guardiola-Diaz, H.M., Rehnmark, S., Usuda, N., Albrektsen, T., Feltkamp, D., Gustafsson, J.A. & Alexson, S.E. (1999) Rat peroxisome proliferator-activated receptors and brown adipose tissue function during cold acclimatization. *J. Biol. Chem.* **274**, 23368-23377.

Gupta, R.K., Vatamaniuk, M.Z., Lee, C.S., Flaschen, R.C., Fulmer, J.T., Matschinsky, F.M., Duncan, S.A. & Kaestner, K.H. (2005) The MODY1 gene HNF-4α regulates selected genes involved in insulin secretion. *J. Clin. Invest.* **115**, 1006-1015.

Hertz, R., Bishara-Shieban, J. & Bar-Tana, J. (1995) Mode of action of peroxisome proliferators as hypolipidemic drugs. Suppression of apolipoprotein C-III. *J. Biol. Chem.* **270**, 13470-13475.

Hinman, L.M. & Blass, J.P. (1981) An NADH-linked spectrophotometric assay for pyruvate dehydrogenase complex in crude tissue homogenates. *J. Biol. Chem.* **256**, 6583-6586.

Huang, B., Wu, P., Bowker-Kinley, M.M. & Harris, R.A. (2002) Regulation of pyruvate dehydrogenase kinase expression by peroxisome proliferator-activated receptor-α ligands, glucocorticoids, and insulin. *Diabetes* **51**, 276-283.

Kamijo, Y., Hora, K., Nakajima, T., Kono, K., Takahashi, K., Ito, Y., Higuchi, M., Kiyosawa, K., Shigematsu, H., Gonzalez, F.J. & Aoyama, T. (2007) Peroxisome proliferator-activated receptor α protects against glomerulonephritis induced by long-term exposure to the plasticizer di-(2-ethylhexyl) phthalate. *J. Am. Soc. Nephrol.* **18**, 176-188.

Lee, S.S., Pineau, T., Drago, J., Lee, E.J., Owens, J.W., Kroetz, D.L., Fernandez-Salguero, P.M.,

Westphal, H. & Gonzalez, F.J. (1995) Targeted disruption of the alpha isoform of the peroxisome proliferator-activated receptor gene in mice results in abolishment of the pleiotropic effects of peroxisome proliferators. *Mol. Cell. Biol.* **15**, 3012-3022.

Lehman, J.J., Barger, P.M., Kovacs, A., Saffitz, J.E., Medeiros, D.M. & Kelly, D.P. (2000) Peroxisome proliferators-activated receptor gamma coactivator-1 promotes cardiac mitochondrial biogenesis. *J. Clin. Invest.* **106**, 847-856.

Mandard, S., Müller, S. & Kersten, S. (2004) Peroxisome proliferators-activated receptor alpha target genes. *Cell. Mol. Life Sci.* **61**, 393-416.

Martin, G., Schoonjans, K., Lefebvre, A. M., Staels, B. & Auwerx, J. (1997) Coordinate regulation of the expression of the fatty acid transport protein and acyl-CoA synthetase genes by PPARα and PPARγ activators. *J. Biol. Chem.* **272**, 28210-28217.

Motojima, K. & Seto, K. (2003) Fibrates and statins rapidly and synergistically induce pyruvate dehydrogenase kinase 4 mRNA in the liver and muscles of mice. *Biol. Pharm. Bull.* **26**, 954-958.

Muoio, D.M., Way, J.M., Tanner, C.J., Winegar, D.A., Kliewer, S.A., Houmard, J.A., Kraus, W.E. & Dohm, G.L. (2002) Peroxisome proliferator-activated receptor-α regulates fatty acid utilization in primary human skeletal muscle cells. *Diabetes* **51**, 901-909.

Nakajima, T., Kamijo, Y., Tanaka, N., Sugiyama, E., Tanaka, E., Kiyosawa, K., Fukushima, Y., Peters, J.M., Gonzalez, F.J. & Aoyama, T. (2004) Peroxisome proliferator-activated receptor α protects against alcohol-induced liver damage. *Hepatology* **40**, 972-980.

O'Farrell, P.H. (1975) High resolution two-dimensional electrophoresis of proteins. *J. Biol. Chem.* **250**, 4007-4021.

Podvinec, M., Kaufmann, M.R., Handschin, C. & Meyer, U.A. (2002) NUBIScan, an *in silico* approach for prediction of nuclear receptor response elements. *Mol. Endocrinol.* **16**, 1269-1279.

Puigserver, P., Wu, Z., Park, C.W., Graves, R., Wright, M. & Spiegelman, B.M. (1998) A cold-inducible coactivator of nuclear receptors linked to adaptive thermogenesis. *Cell* **92**,

829-839.

Schoonjans, K., Peinado-Onsurbe, J., Lefebvre, A. M., Heyman, R. A., Briggs, M., Deeb, S., Staels, B. & Auwerx, J. (1996) PPARα and PPARγ activators direct a distinct tissue-specific transcriptional response via a PPRE in the lipoprotein lipase gene. *EMBO J.* **15**, 5336-5348.

Shindo, Y., Osumi, T. & Hashimoto, T. (1978) Effects of administration of di-(2-ethylhexyl) phthalate on rat liver mitochondria. *Biochem. Pharmacol.* **27**, 2683-2688.

Tanaka, N., Moriya, K., Kiyosawa, K., Koike, K., Gonzalez, F.J. & Aoyama, T. (2008) PPAR α activation is essential for HCV core protein-induced hepatic steatosis and hepatocellular carcinoma in mice. *J. Clin. Invest.* **118**, 683-694.

Toda, T. (2000) Current status and perspectives of proteomics in aging research. *Exp. Gerontol.* **35**, 803-810.

Tong, Y., Hara, A., Komatsu, M., Tanaka, N., Kamijo, Y., Gonzalez, F.J. & Aoyama, T. (2005) Suppression of expression of muscle-associated proteins by PPARα in brown adipose tissue. *Biochem. Biophys. Res. Commun.* **336**, 76-83.

Vega, R.B., Huss, J.M. & Kelly, D.P. (2000) The coactivator PGC-1 cooperates with peroxisome proliferators-activated receptor α in transcriptional control of nuclear genes encoding mitochondrial fatty acid oxidation enzymes. *Mol. Cell. Biol.* **20**, 1868-1876.

Vega, R.B. & Kelly, D.P. (1997) A role for estrogen-related receptor α in the control of mitochondrial fatty acid β-oxidation during brown adipocyte differentiation. *J. Biol. Chem.* **272**, 31693-31699.

Watanabe, K., Fujii, H., Takahashi, T., Kodama, M., Aizawa, Y., Ohta, Y., Ono, T., Hasegawa, G., Naito, M., Nakajima, T., Kamijo, Y., Gonzalez, F.J. & Aoyama, T. (2000) Constitutive regulation of cardiac fatty acid metabolism through peroxisome proliferator-activated receptor alpha associated with age-dependent cardiac toxicity. *J. Biol. Chem.* **275**, 22293-22299.

Yu, X.X., Lewin, D.A., Forrest, W. & Adams, S.H. (2002) Cold elicits the simultaneous induction of fatty acid synthesis and beta-oxidation in murine brown adipose tissue: prediction from differential gene expression and confirmation in vivo. *FASEB J.* **16**, 155-168.

Figure legends

Figure 1 Proteomic analyses of BAT. (A) SDS-PAGE analysis of BAT obtained from PPARα-null and wild-type mice. The protein samples obtained from 20 mg of interscapular BAT were loaded onto a re-swollen Immobiline DryStrip, respectively. The proteins were separated by IEF, followed by 2D SDS-PAGE. The samples from PPARα-null mice and wild-type controls were simultaneously analyzed using the same apparatus. The spot is indicated by an arrow on the gel. kDa, kilodalton; IEF, isoelectric focusing. (B) The MALDI-TOF-MS spectrum of the tryptic peptides obtained from the spot. Interscapular BAT of PPARα-null mice was analyzed by 2D SDS-PAGE, as shown in Fig. 1A, and the spot was excised and digested overnight at 30ºC using a Montage In-Gel $Digest_{96}$ Kit containing trypsin. Peptides were extracted from the gels and purified with $ZipTip_{C18}$. Finally, the purified peptides were eluted from $ZipTip_{C18}$ and analyzed by MALDI-TOF-MS in the reflector mode. The numbers at the top of each peak indicate the molecular mass.

Figure 2 Changes in BAT weight, its histological analyses, and triglyceride contents under cold acclimatization. (A) The ratios of the BAT weight to body weight at 1, 2, 4, 8, and 12 weeks under constitutive (23ºC) or cold conditions (4ºC). White and black marks indicate wild-type and PPARα-null mice, respectively. (B) Histological analyses of BAT at 8 weeks under constitutive or cold conditions. Small sections of BAT from each mouse were fixed in 10% buffered formalin, and the sections were stained with H&E. Scale bar at the lower right corner of the lower right photograph, 20 μm. (C) Triglyceride content in BAT at 8 weeks under constitutive or cold conditions. White and black bars indicate wild-type and PPARα-null mice, respectively. Values are presented as means ± SD (n = 5). *: significant difference (P<0.05) between 23ºC vs. 4ºC, $^{\#}$: significant difference (P<0.05) between wild type vs. PPARα-null mice.

Figure 3 The expression of typical enzymes of the glucose degradation system and PDH activity under constitutive or cold conditions. (A) The mRNA content of PDHα, PDHβ, PDK2, and PDK4 under constitutive (23ºC) or cold conditions (4ºC). (B) The mRNA content of PC, M-PK, and HK-II under constitutive (23ºC) or cold conditions (4ºC). (C) PDH activity under constitutive or cold conditions. PDH activity was measured using the method of Hinman and Blass (Hinman & Blass, 1981). White and black bars indicate wild-type and PPARα-null mice, respectively. Values are presented as means ± SD (n = 5). *: significant difference (P<0.05) between 23ºC vs. 4ºC, $^{\#}$: significant difference (P<0.05) between wild type vs. PPARα-null mice.

Figure 4 The **expression of typical proteins in fatty acid metabolizing system and the related nuclear proteins.** The mRNA content of LACS, CPT1b, and MCAD (A), FAT, FATP, and LPL (C), ACC-1 and FAS (D), and PPARα, PPARγ, HNF4α, and PGC-1α (E) under constitutive (23ºC) or cold conditions (4ºC). (B) Palmitic acid β-oxidation activity under constitutive or cold conditions. Fatty acid β-oxidation activity was measured as follows (Shindo *et al.*, 1978). BAT was homogenized in four volumes of 0.25 M sucrose containing 1 mM EDTA. Homogenate was incubated with the assay medium containing 50 μM [1-^{14}C]palmitic acid. Radioactive degradation products were measured after the removal of unreacted substrate. White and black bars indicate wild-type and PPARα-null mice, respectively. Values are presented as means ± SD (n = 5). *: significant difference (P<0.05) between 23ºC vs. 4ºC, $^{\#}$: significant difference (P<0.05) between wild type vs. PPARα-null mice.

Figure 1

A SDS-PAGE analysis of BAT

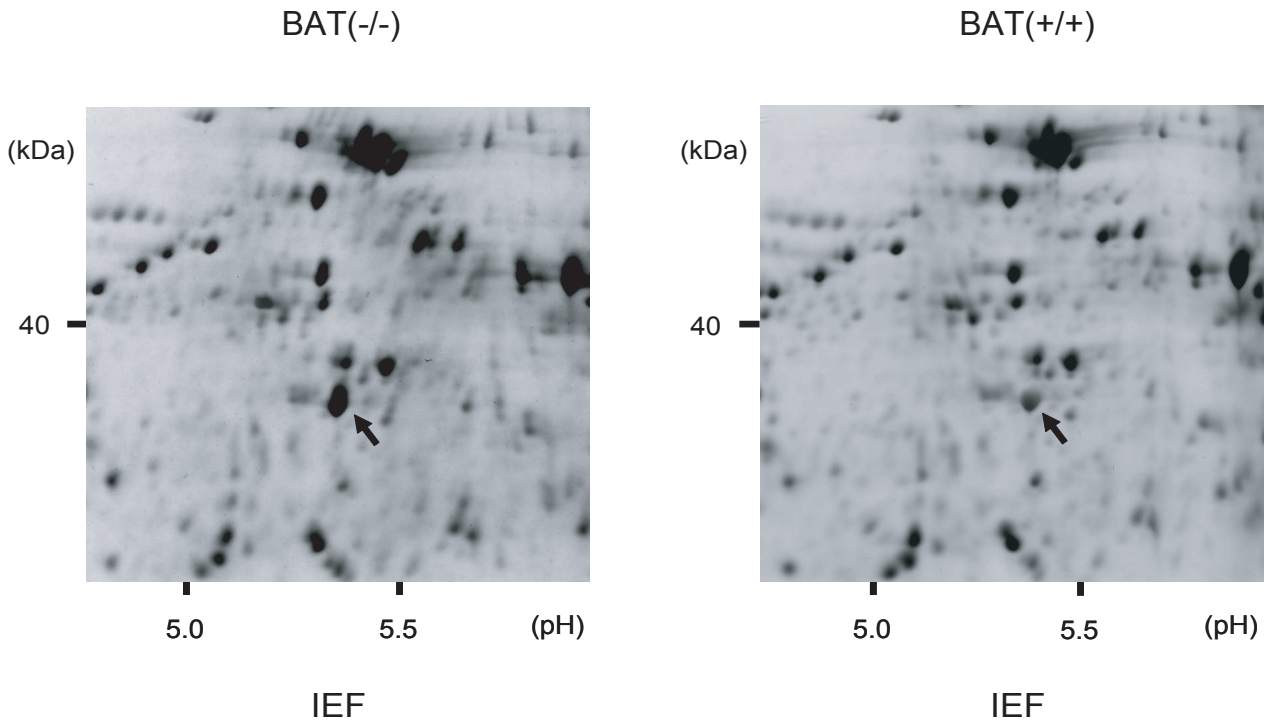

B MALDI-TOF-MS spectrum

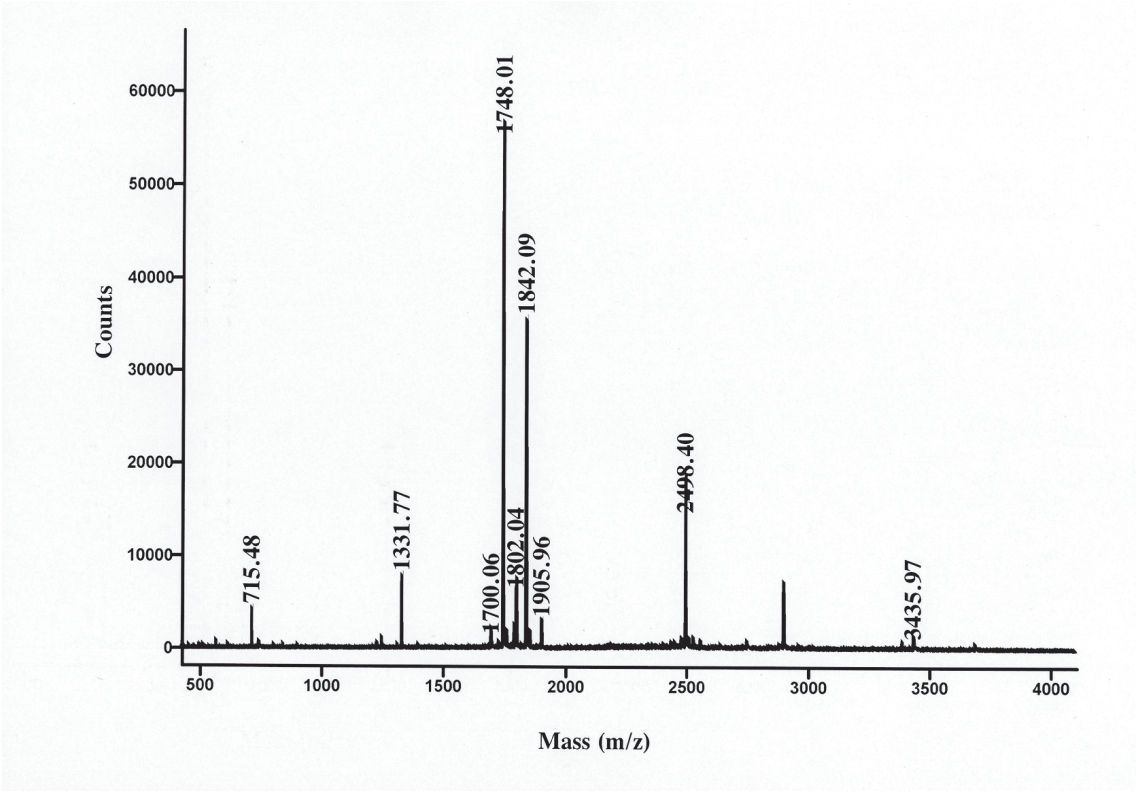

Figure 2

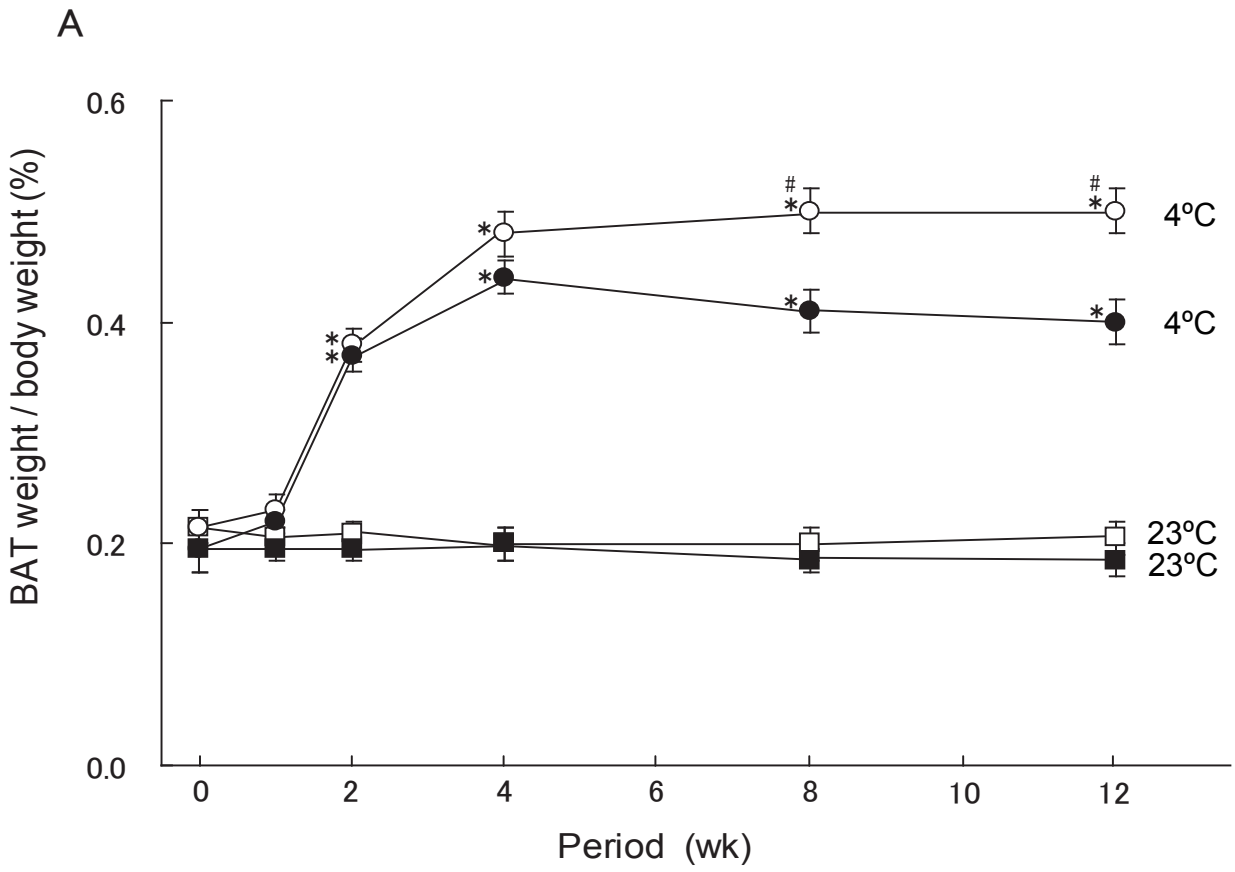
A
BAT weight / body weight (%)
0.6
0.4
0.2
0.0
0
2
4
6
8
10
12
Period (wk)
4ºC
4ºC
23ºC
23ºC

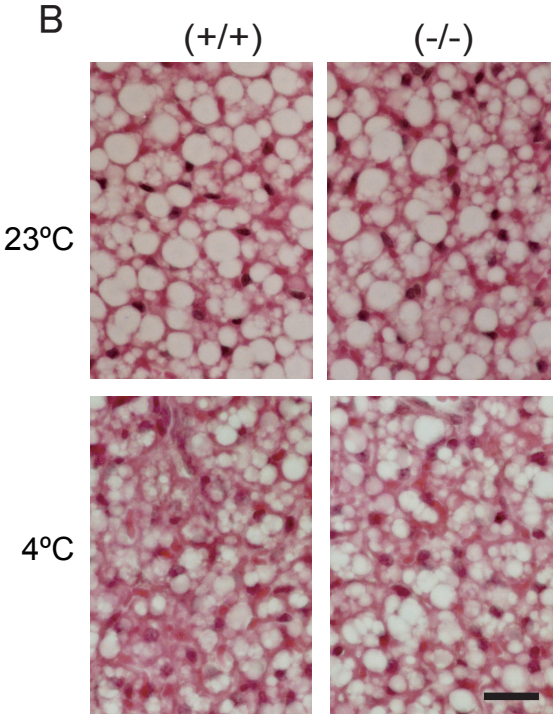
B
(+/+)
(-/-)
23ºC
4ºC

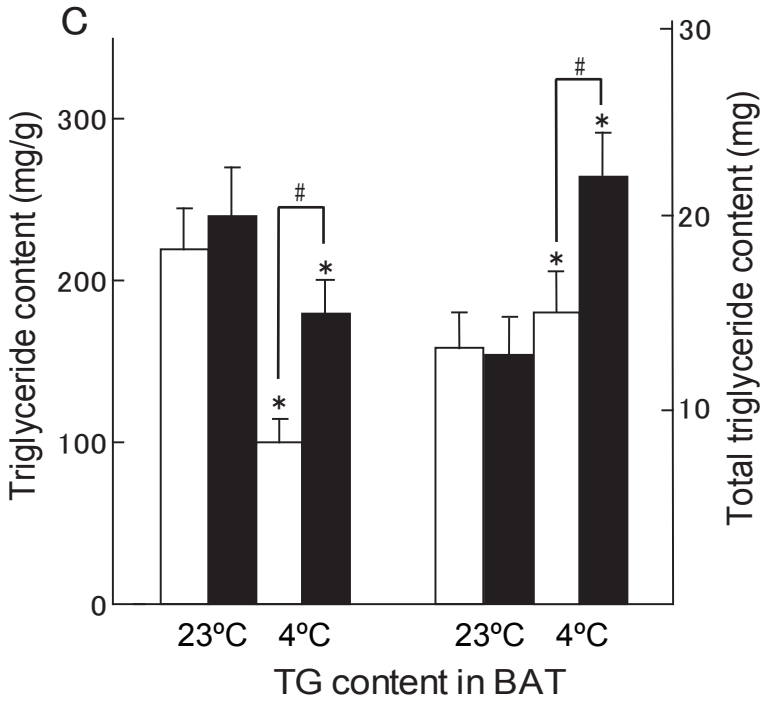
C
Triglyceride content (mg/g)
300
200
100
0
Total triglyceride content (mg)
30
20
10
23ºC
4ºC
23ºC
4ºC
TG content in BAT

Figure 3

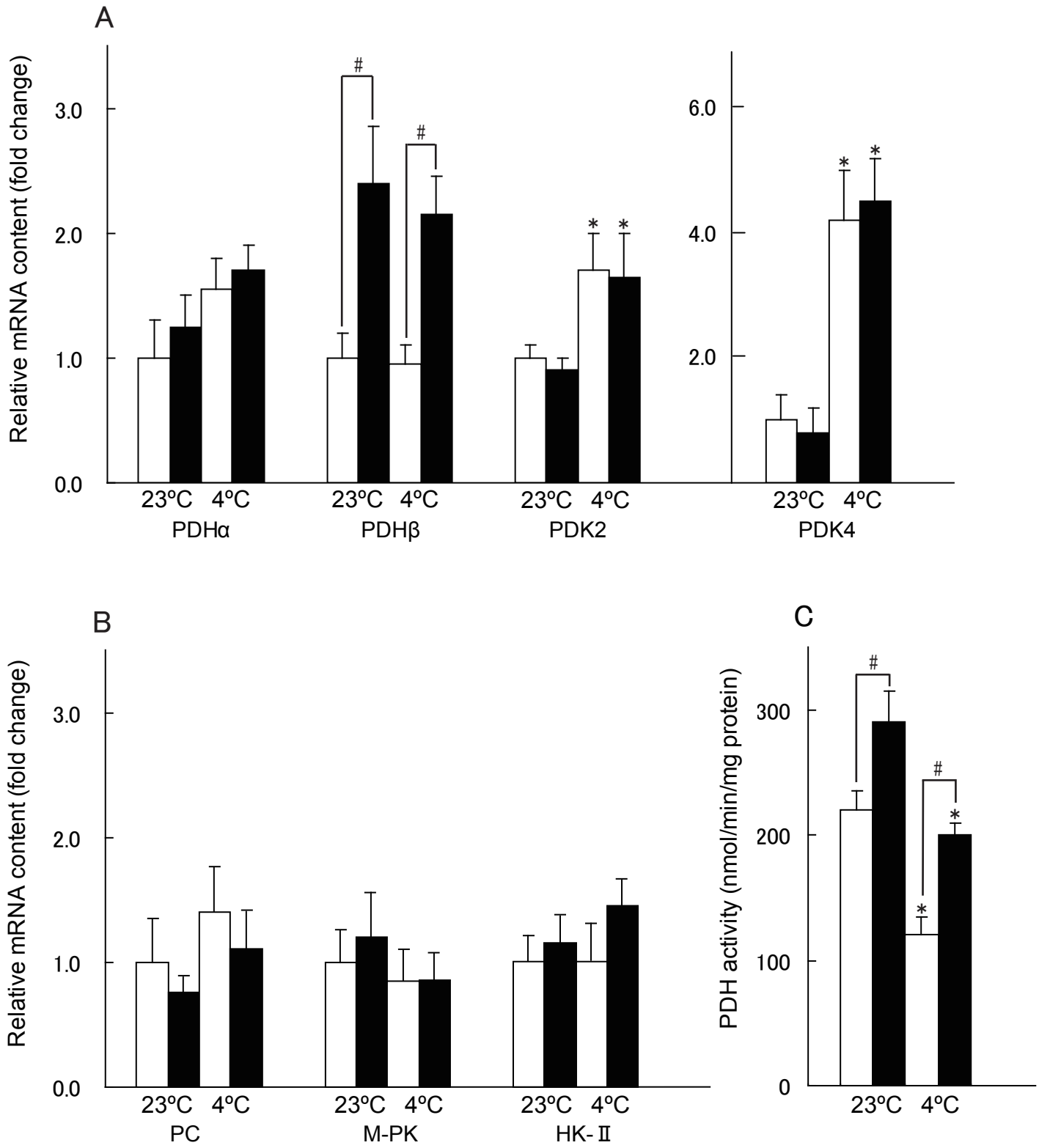
A
Relative mRNA content (fold change)
3.0
2.0
1.0
0.0
6.0
4.0
2.0
#
#
*
*
*
*
23ºC 4ºC
PDHα
PDHβ
PDK2
PDK4
B
Relative mRNA content (fold change)
3.0
2.0
1.0
0.0
PC
M-PK
HK-Ⅱ
C
PDH activity (nmol/min/mg protein)
300
200
100
0
#
#
*
*
23ºC 4ºC

Figure 4

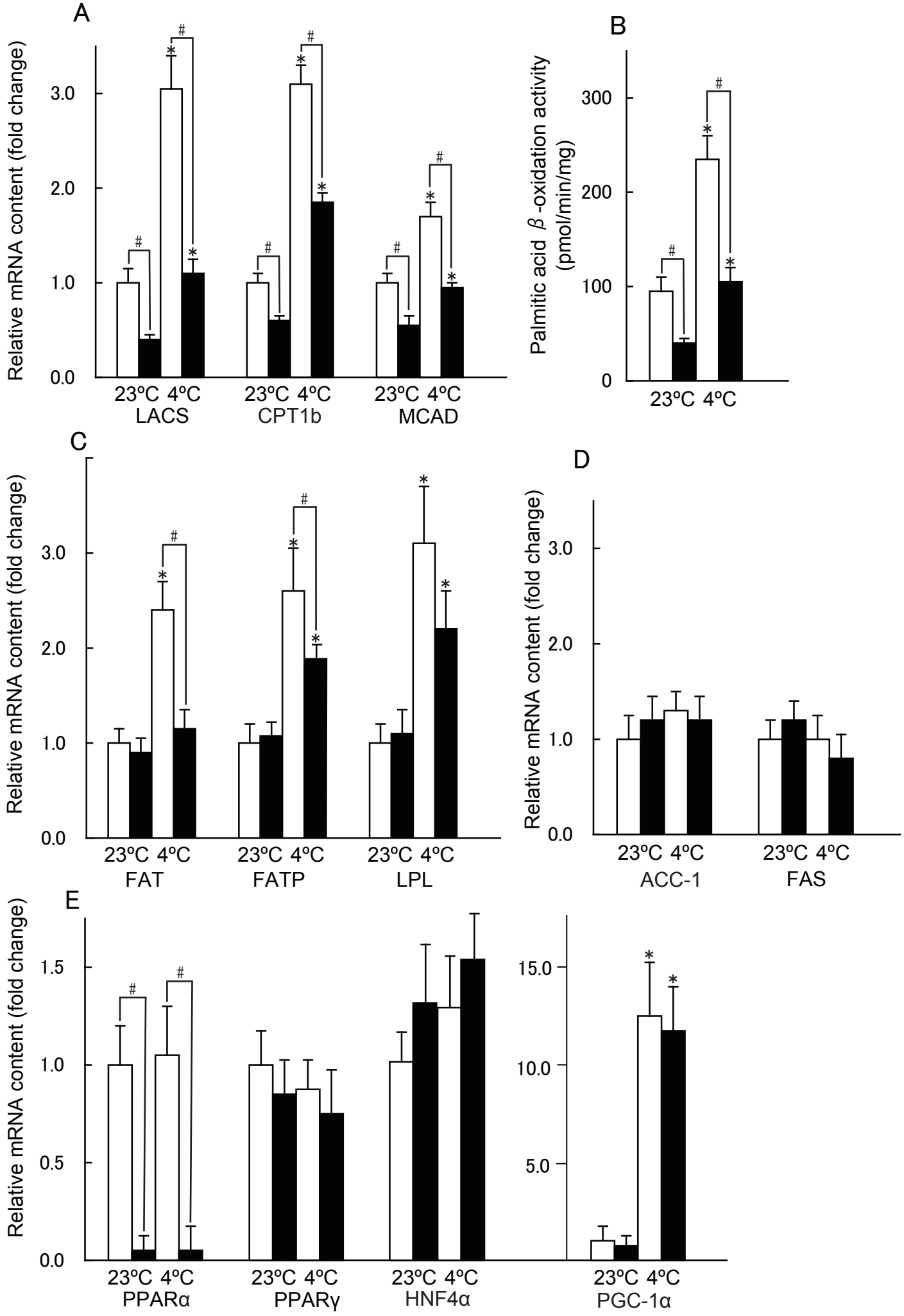
A
Relative mRNA content (fold change)
3.0
2.0
1.0
0.0
23ºC 4ºC
LACS
23ºC 4ºC
CPT1b
23ºC 4ºC
MCAD
B
Palmitic acid β-oxidation activity
(pmol/min/mg)
300
200
100
0
23ºC 4ºC
C
Relative mRNA content (fold change)
3.0
2.0
1.0
0.0
23ºC 4ºC
FAT
23ºC 4ºC
FATP
23ºC 4ºC
LPL
D
Relative mRNA content (fold change)
3.0
2.0
1.0
0.0
23ºC 4ºC
ACC-1
23ºC 4ºC
FAS
E
Relative mRNA content (fold change)
1.5
1.0
0.5
0.0
23ºC 4ºC
PPARα
23ºC 4ºC
PPARγ
23ºC 4ºC
HNF4α
15.0
10.0
5.0
23ºC 4ºC
PGC-1α